Moroccan Journal of Chemistry
ISSN: 2351-812X
http://revues.imist.ma/?journal=morjchem&page=login
Thai Anh Nguyen & al. / Mor. J. Chem. 9 N°1 (2021) 018-027

Batch and column adsorption of reactive dyes by eggshell powder–chitosan gel core-shell material

Thai Anh Nguyen[(a)], Vinh Tien Nguyen[(a)]*, Thi Thanh Hieu Tran[(a)], Thi Quynh Nhu Le[(a)], Nhat Huy Nguyen[(b)]

[(a)] *Faculty of Chemical and Food Technology, Ho Chi Minh City University of Technology and Education, Ho Chi Minh City, Vietnam*

[(b)] *Faculty of Environment and Natural Resources, Ho Chi Minh City University of Technology, VNU-HCM, Ho Chi Minh City, Vietnam*

** Corresponding author:*
tiennv@hcmute.edu.vn
Received 23 Feb 2020,
Revised 26 Sep 2020,
Accepted 03 Nov 2020.

Abstract

In this study, eggshell powder-chitosan gel (EPCG) material was synthesized and tested as an adsorbent for two commercial reactive dyes in batch and dynamic modes. The EPCG material was a novel core-shell material in which the eggshell core particles were coated by a thin layer of chitosan. SEM images of dried EPCG powder showed a porous structure of the surface. In adsorption batch tests, Langmuir and Freundlich equations well described the adsorption isotherms with a maximum capacity of 2.3 mg/g at pH 4 and equilibrium time of 60 min (r^2> 0.98). The adsorption process followed pseudo-second-order kinetics. Adsorption behaviour of EPCG toward the reactive dyes in fixed-bed adsorber was better described by the Clark model (r^2> 0.92) than by the Bohart – Adam model (r^2> 0.82). These results suggest that EPCG, as an environment-friendly material produced from waste eggshell, is very promising for wastewater treatment applications.

Keywords: *Reactive dyes; Eggshell; Chitosan; Clark model; Fixed-bed column.*

1. Introduction

Dyes and pigments are one of the most popular water pollutants emitted from various industries [1, 2]. Wastewater from the textile dyeing usually contains about 8–20% original dyes and other toxic chemicals. Reactive dyes (e.g. azo dyes) are the most common dyes containing various chemicals such as substituted heterocyclic and aromatic compounds [3], which are toxic to the aquatic environment. Moreover, the removal of reactive dyes by conventional physicochemical or biological treatments is facing many difficulties due to their high aqueous solubility. In this case, adsorption is emerging as a convenient and effective technology for the treatment of dyes in wastewater [4]. Practically, activated carbon is widely used although it is relatively expensive [5]. Recently, many new and low-cost adsorbents such as natural materials, biosorbents, industrial and agriculture waste materials, chitosan, and calcinated mussel shells have been developed and applied for dyes removal [2]. Eggshell, a popular waste from food industries with high quantity, has been proved as a natural sorbent for the removal of coloured dyes and phenolic compounds in wastewater [6]. Eggshell comprises of $CaCO_3$ layers with many functional groups such as –OH, -C=O, $–PO_4$, amines, and amides, which are potential for the adsorption process [7]. Depend on solution pH, the surface of eggshell could contain positively charged due to its $–NH_3$ and $–CO–N^+H_2–$ functional groups [8]. In literature, adsorption tests have been investigated for reactive yellow 2 (RY2) and reactive black 5 (RB5) by chitosan [3, 9] and eggshell [10, 11]. To our knowledge, there has not been any work combining the advantages of both chitosan and eggshell for removal of reactive dyes in wastewater. This study aims to synthesize a novel dried eggshell powder-chitosan gel (EPCG) material and investigate its feasibility for removal of commercial reactive dyes from aqueous solution. Both batch and fixed-bed column adsorption tests were investigated. The parameters obtained from adsorption kinetics, isotherms and column modelling were also evaluated and discussed.

2. Materials and methods

2.1. Materials

Waste eggshells were collected from a local bakery workshop (Ho Chi Minh City, Vietnam), washed thoroughly by tap water, rinsed with distilled water several times, and dried in an oven at 60 ^oC for 12 h. Eggshell membranes were then carefully removed and the remaining solids were mechanically granulated by a crusher, screened by sieves of 0.15 mm, and stored in a desiccator for further experiments. Two commercial reactive dyes including Suncion Red H_R (SRH-R) and Sunzol Blue RS (SB-RS) were purchased from Ohyoung Inc. (Korea). Other chemicals were obtained from Sigma Chemical Co. (USA). Chitosan powder was purchased from VNChitosan Co. Ltd, (Vietnam).

2.2. Experimental methods

2.2.1. Preparation of adsorbent

A chitosan solution was prepared by dissolving 0.5 g of chitosan in 7 mL of 8% (w/w) aqueous acetic acid. The obtained chitosan solution was mixed thoroughly with 5.5 g of eggshell powder and then added drop-wise into a coagulating solution of H_2O:methanol:1N NaOH solution with a volume ratio of 150:125:50 under continuous stirring. The produced material was kept in the coagulating solution for 10 min, then picked up, and washed with 10% (w/w) H_2SO_4 solution, followed by washing with distilled water until neutral pH. The obtained material was finally dried at 60 ^oC for 12 h, desiccated for 2 h, and cut into 2.5 mm pieces.

2.2.2. Batch adsorption tests

Preliminary experiments were conducted to determine effective dosages of EPCG for 50 mL of SRH-R and SB-RS solutions with different concentrations ranging from 10 to 50 mg/L and pH from 2.0 to 9.0. The effective dosages

were 0.8 g for SRH-R and 1.8 g for SB-RS in a H_2SO_4 solution with pH 3. The solution was placed in a rotary incubator shaker at 250 rpm and 30 °C to ensure adsorption equilibrium. Samples of the dye solution were collected at predetermined intervals of time and filtered to analyze the concentration of the remaining dye by measuring absorbance at 542 nm for SRH-R and 624 nm for SB-RS. All the experiments were conducted in triplicate, and the average results are used for calculations. The amount of dye adsorbed on the EPCG at some moment t (q_t, mg g^{-1}) is calculated as followed:

$$q_t = \frac{(C_0 - C_t) \times V}{m} \quad (1)$$

where V (L) is the volume of the solution and m (g) is the weight of EPCG used. C_o and C_t (mg/L) are the concentrations of the dye at the beginning and the moment t, respectively. To reveal the kinetic characteristics and possible mechanisms of adsorption, the experimental data were fitted to Lagergren's pseudo-first-order, pseudo-second-order and intra-particle diffusion models [12]. The linear forms of these models are expressed as follow:

Pseudo-first-order model: $\ln(q_e - q_t) = \ln q_e - k_1 t$ (2)

Pseudo-second-order model $\frac{t}{q_t} = \frac{1}{k_2 q_e^2} + \left(\frac{1}{q_e}\right) t$ (3)

Intraparticle diffusion model: $q_t = K_i t^{0.5} + I$ (4)

In these equations, q_t and q_e (mg g^{-1}) are the amount of dye adsorbed on adsorbent at time t (min) and at equilibrium, respectively; k_1 (min^{-1}), k_2 (g mg^{-1} min^{-1}) and K_i are the pseudo-first-order, pseudo-second-order and intraparticle-diffusion rate constants, respectively; I is the intraparticle diffusion model constant.

2.2.3. Fixed-bed column adsorption tests

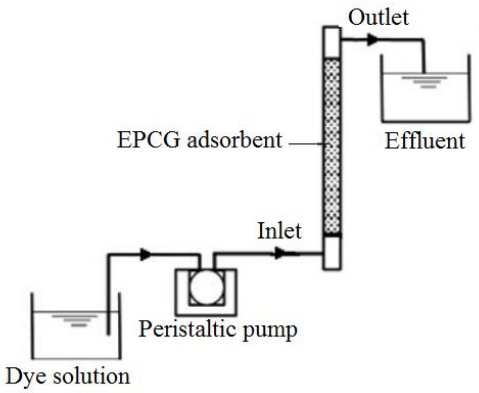

Figure 1. Schematic representation of the fixed-bed column adsorption tests in upflow mode.

To determine the efficiency of reactive dyes adsorption onto EPCG, continuous-flow adsorption experiments were also performed in a glass column with an internal diameter of 1 cm. The column was packed with EPCG (15 cm of height) and upflow mode was applied for the inlet flow (5, 8 and 11 mL/min) of the dye solutions (25 and 50 mg/L) at 30 °C and pH 3.0 (Figure 1). Dye concentration in the effluent was determined over time by measuring the absorbance of the effluent. The breakthrough curves were expressed as the ratio of effluent to influent concentrations (C_t/C_0) as a function of time (t). From each breakthrough curves, breakthrough point (the moment that outlet concentration of the dye reached 1% of the inlet concentration), and exhausted point (the moment that outlet concentration reached 90% of

inlet concentration). These results are important characteristics of the operation, dynamic response, and process design of a sorption column [13].

3. Results and Discussions

3.1. Characterization of the EPCG adsorbent

SEM images of the EPCG adsorbent surface before and after adsorption tests are shown in Figure 2. The porous and rough structure of the EPCG is easily recognized in Figure 2a, which is very advantageous for adsorption applications. The surface structure of EPCG changed after dye adsorption, as observed in Figure 2b. On the surface of dye-adsorbed EPCG, the rippled and rough surface became a smoother and tighter structure, proving the effective adsorption of dye via a stable dye layer on the surface of EPCG material.

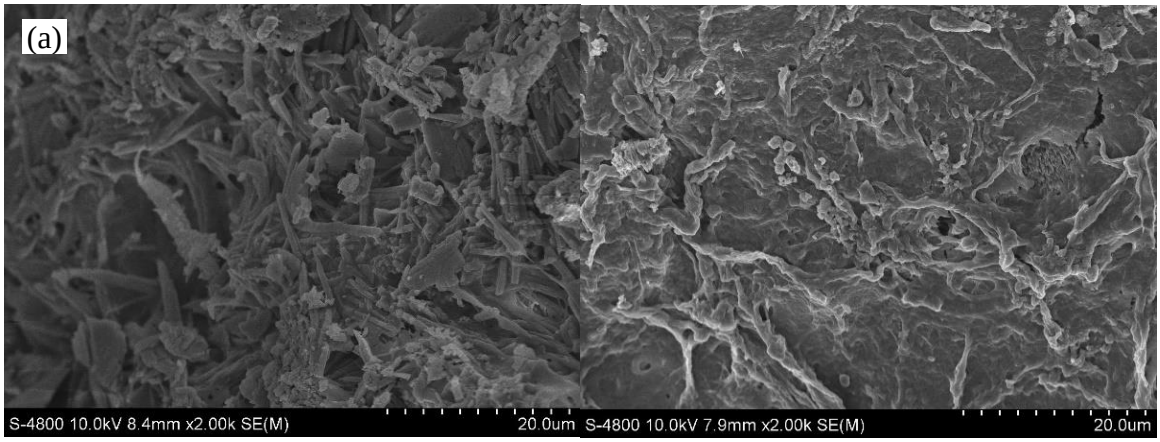

Figure 2. SEM images of EPCG (a) before and (b) after dye adsorption.

FTIR spectra in Figure 3 further demonstrate the structural changes of the EPCG as a result of dye adsorption on EPCG surface. Chitosan is identified by the presence of a peak at 3402.2 cm^{-1} and other common peaks at approximately 3200 to 3600 cm^{-1} due to –OH and $–NH_2$ stretching vibrations [14]. Peaks at 711.68 cm^{-1} and 875.62 cm^{-1} correspond to P–O and S=O stretching vibrations while the band at 1417.58 cm^{-1} denotes C=O stretching vibration. This further clarifies that calcite is the fundamental constituent of the eggshell [6]. After adsorption of reactive dyes, there are slight changes in the peak shape at 3402.2 cm^{-1}, the band at 1150-1093 cm^{-1} and the peak height at 601.76 cm^{-1} due to the interaction between the adsorbed reactive dye and the EPCG material [15].

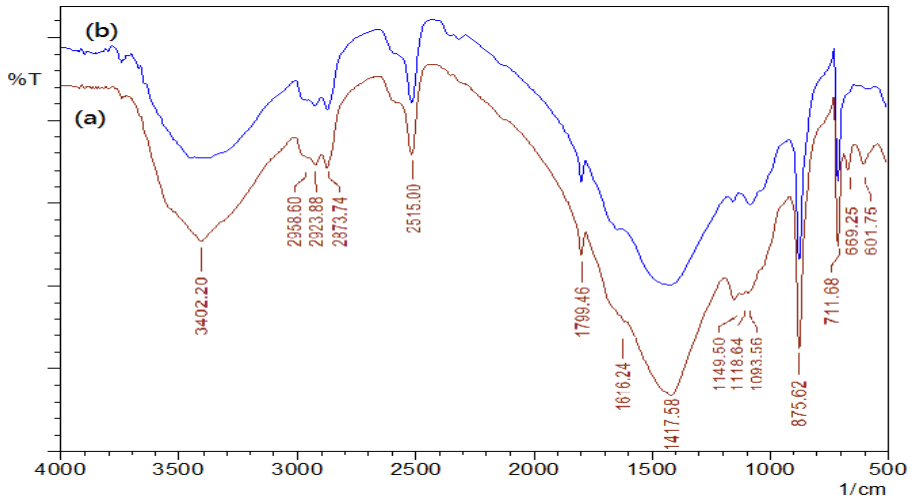

Figure 3. FTIR spectra of EPCG (a) before and (b) after dye adsorption.

3.2. Kinetic adsorption study

To design any full-scale batch adsorption process, determination of adsorption rate, as well as the rate-determining step are important. Adsorption kinetics can be controlled by different mechanisms, including liquid film diffusion, pore diffusion or chemical interaction. The chemical interaction can occur between the functional groups on the chitosan gel surface and the dye molecules via complexation or ion exchange. The conformity between the experimental results and the models is usually evaluated based on the determination coefficient R^2.

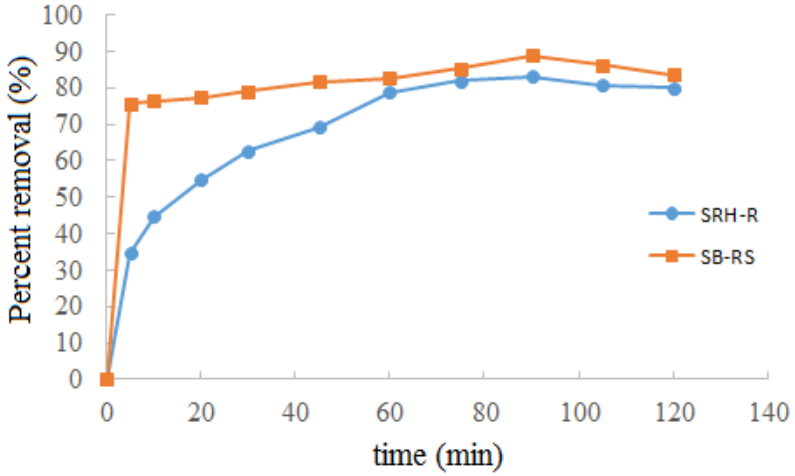

Figure 4. Removal of dyes over time from aqueous solution by adsorption on EPCG. The initial concentration of dyes: 10 mg/L.

The pseudo-first-order kinetic model is based on the assumption that the adsorption rate is proportional to the number of free adsorption sites of the adsorbent. This model is equivalent to the diffusion expression for the case of dye diffusion through a liquid film surrounding adsorbent particles. The pseudo-second-order model is based on the assumption that chemical reaction between adsorbent and adsorbate (chemisorption) is the rate-determining step, while the intraparticle diffusion model assumes that the diffusion of adsorbate molecules in the pore [16, 17]. After fitting the kinetic experimental data into the three models (data not shown), the pseudo-second-order (PSO) model showed the best fitting with the highest values of r^2 (Table 1). The half-life ($t_{1/2}$) is the time for EPCG to adsorb a half of the initial amount of the dye in solution and can serve for evaluating the operating time of an adsorptive system. Half-life values of SRH-R were smaller than those of SB-RS, indicating that the adsorption process of SRH-R occurred more quickly than that of SB-RS.

Table 1. Parameters of the pseudo-second-order kinetic model for adsorption of reactive dyes on EPCG.

	C_0 ($mg{\cdot}L^{-1}$)	$q_{e,cal}$ ($mg{\cdot}g^{-1}$)	k_2 ($g.mg^{-1}.min^{-1}$)	$\mathbf{t_{1/2}}$ (min)	r^2
SRH-R	10	0.460	0.192	11.3	0.9898
	20	0.870	0.099	11.6	0.9970
	30	1.410	0.038	18.7	0.9569
SB-RS	10	0.558	0.057	31.4	0.9748
	20	0.906	0.035	31.5	0.9509
	30	1.373	0.023	31.7	0.9474

3.3. Adsorption equilibrium modelling

Langmuir and Freundlich equations were selected in this work to elucidate adsorption mechanisms. The linearized form of the Langmuir and Freundlich equations are given as following [18-20]:

$$\frac{C_e}{q_e} = \frac{1}{q_{\max} \times K_L} + \frac{C_e}{q_{\max}} \quad (5)$$

$$\ln q_e = \ln K_F + \left(\frac{1}{n}\right) \ln C_e \quad (6)$$

where q_{max} (mg/g) is the maximum adsorption capacity corresponding to complete monolayer coverage and K_L (L/mg) is the Langmuir constant. K_F is the Freundlich constant ($mg^{1-(1/n)}$ $L^{1/n}/g$) related to the adsorption capacity and the constant n is related to the adsorption intensity.

Table 2. Isotherm constants for the adsorption of reactive dyes on EPCG at 30 °C.

	Dye	q_{max} ($mg \cdot g^{-1}$)	K_L ($L \cdot mg^{-1}$)	r^2
Langmuir	SRH-R	2.794	0.068	0.9908
	SB- RS	2.948	0.151	0.9598
	Dye	n	K_F	r^2
Freundlich	SRH-R	1.6323	0.260	0.9883
	SB- RS	1.95	0.517	0.9924

In SEM images, the surface of the adsorbent has a porous and rough shape which is suitable for physical adsorption. The values of r^2 in Table 2 indicated that equilibrium adsorption of SRH-R was better fitted with the Langmuir model (0.9908 > 0.9883), while adsorption of SB-RS was better fitted with the Freundlich model (0.9924 > 0.9598). The n values in the Freundlich model for both dyes were larger than 1, indicating favoured adsorption [21]. These results reveal the high capable adsorption of this adsorbent for reactive dyes. The q_{max} values in this study (Table 2) were higher (i.e., 1.29 to 2.3 fold) than those reported in a previous paper where only eggshell without chitosan [11]. It is possibly due to the polymeric nature and the functional groups (-OH, $-NH_2$, $-CONH_2$) enhanced the interaction between EPCG with the reactive dyes. Furthermore, additional adsorption experiments were also done with the activated carbon and the same reactive dyes under the same conditions. The results in Figure 5 showed that EPCG had comparable adsorbing capacity with activated carbon towards these reactive dyes.

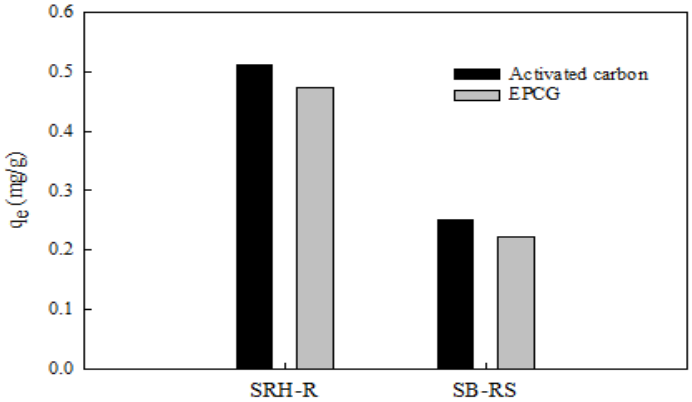

Figure 5. Adsorption capacity of activated carbon and EPCG for SRH-R and SB-RS dyes.

3.4. Adsorption column modelling

Column adsorption (i.e. in fixed-bed adsorber) is the most common and efficient way for the purification of water and wastewater. It is generally accepted that a bed-depth service time model (BDST) offers the simplest approach and rapid prediction of adsorber design and performance. The basic relations that relate C_0/C_b and column service time (t) for purification in a flowing system were proposed by Bohart and Adams, originally developed for the removal of chlorine gas by charcoal column [22]. However, its overall approach was successfully applied in the quantitative description of many adsorption systems. This model assumes that the adsorption rate is proportional to both the residual capacity of adsorbent and the concentration of the adsorbing solute, as presented in Equation (7). Equation (8) is the reduced form of Equation (7) when the exponential term is frequently much larger than 1 [23]:

$$\ln\left(\frac{C_0}{C_b}-1\right)=\ln\left(e^{k_a N_0 H/u}-1\right)-k_a C_0 t \quad (7)$$

$$t=\frac{N_0}{C_0 u}H-\frac{1}{k_a C_0}\ln\left(\frac{C_0}{C_b}-1\right) \quad (8)$$

In these formulae, C_0 and C_b ($kg{\cdot}m^{-3}$) are the inlet and the breakthrough dye concentration, respectively; t (min) is the service time; H (m) is the bed-depth; N_0 ($kg{\cdot}m^{-3}$) is the column adsorption capacity; u (m/min) is the linear flow rate of dye solution; k_a (m^3 /(kg.min)) is the BDST rate constant. The values of k_a and N_0 can be determined by plotting $\ln[(C_0/C_b) -1]$ vs. time (Table 3 and Figure 6). The parameters of Bohart and Adams model in Table 3 were calculated at 90% of column exhaustion and 40% breakthrough point. Besides, the slope of the straight line ($N_0/(C_0.u)$) in Equation (8) implies that 0.33 hr is needed to exhaust 1.0 cm of adsorbent bed during adsorption of reactive dyes at 50% breakthrough. The value of N_0 in kg/m^3 is 0.01407 (Table 3) and in kg/kg units is 0.000025 when the bulk density of the adsorbent is 570 kg/m^3. The N_0 value of $2.5{\cdot}10^{-5}$ implied that only 20.72% of the available adsorbent capacity (0.002794 kg/kg in Table 2) was applied in the adsorber at 50% breakthrough point.

Table 3: Effect of initial reactive dyes concentration and volumetric flow rate on the parameters of the Bohart and Adams model.

C_0	F	SRH-R				SB-RS			
		N_0	$N_0/(C_0.u)$	k_a	r^2	N_0	$N_0/(C_0.u)$	k_a	r^2
	5	0.01407	0.33	0.092	0.9358	0.01406	0.33	0.08	0.8132
0.025	8	0.01245	0.29	0.116	0.9531	0.01637	0.39	0.076	0.849
	11	0.00903	0.21	0.184	0.9754	0.01209	0.29	0.128	0.9422
	5	0.01013	0.12	0.096	0.9137	0.01469	0.17	0.092	0.8618
0.050	8	0.00925	0.11	0.128	0.9455	0.00893	0.11	0.116	0.8929
	11	0.00809	0.10	0.172	0.9732	0.00759	0.09	0.164	0.9399

Note: C_0(kg/m^3); F (mL/min); k_a (m^3/kg/min); N_0 (kg/m^3); $N_0/(C_0.u)$ (hr/cm)

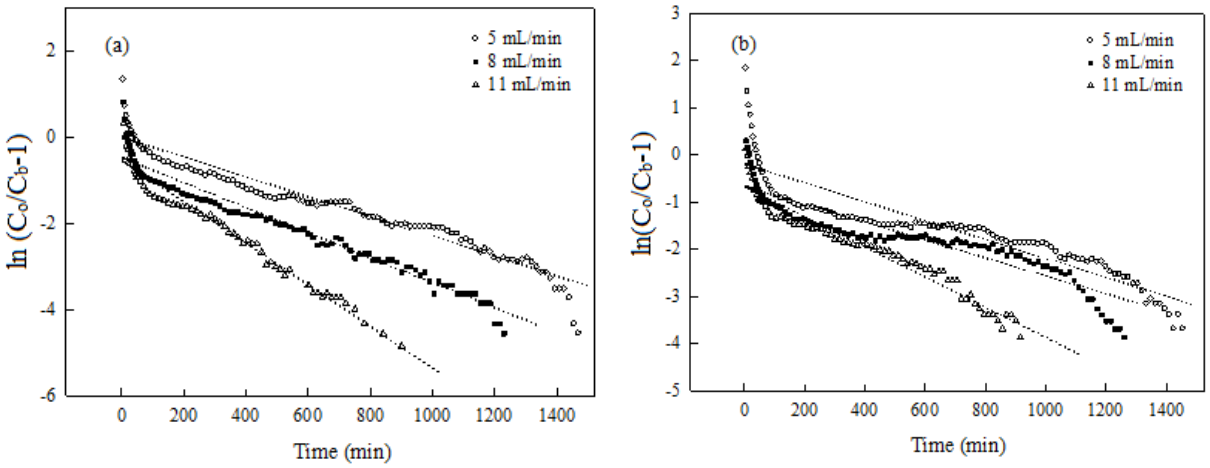

Figure 6. The Adams–Bohart model's linear form of (a) SRH-R and (b) SB-RS adsorption. Dye concentration = 25 mg/L, pH 4.0 T=30 °C.

Another model for column test, developed by Clark, is based on the use of a mass transfer concept in combination with the Freundlich isotherm [24]:

$$\ln\left[\left(\frac{C_0}{C_t}-1\right)^{n-1}-1\right]=\ln A-\omega t \qquad (9)$$

In this equation, C_t and C_0 (mg/L) are the influent and effluent concentrations, respectively; n is the parameter in the Freundlich isotherm; A and ω are the Clark constants. Equation (9) was applied to the effluent data for the fixed-bed adsorber using linear regression. Values of ω (1/h) and A can be determined from the plot of $\ln[(C_0/C_t)^{n-1}-1]$ vs. time (Figure 7 and Table 4). The data from the fixed bed column studies was better fitted by Clark model ($r^2>0.9229$) (Table 3 and 4). As the bed depth increased and both the influent concentration and the flow rate increased, the values of r (1/h) increased, indicating an increase in the adsorption speed.

Table 4. Effect of initial reactive dyes concentration and volumetric flow rate on the parameters of Clark model.

C_0	F	SRH-R			SB-RS		
(mg/L)	(mL/min)	lnA	ω (1/h)	r^2	lnA	ω	r^2
	5	0.5945	0.0022	0.9397	0.5945	0.0022	0.9397
25	8	1.0197	0.0029	0.9569	1.0197	0.0029	0.9569
	11	1.1243	0.0032	0.9763	1.1243	0.0032	0.9763
	5	0.9729	0.0023	0.9229	0.9729	0.0023	0.9229
50	8	1.2845	0.0023	0.9487	1.2845	0.0023	0.9487
	11	1.3293	0.0043	0.9756	1.3293	0.0043	0.9756

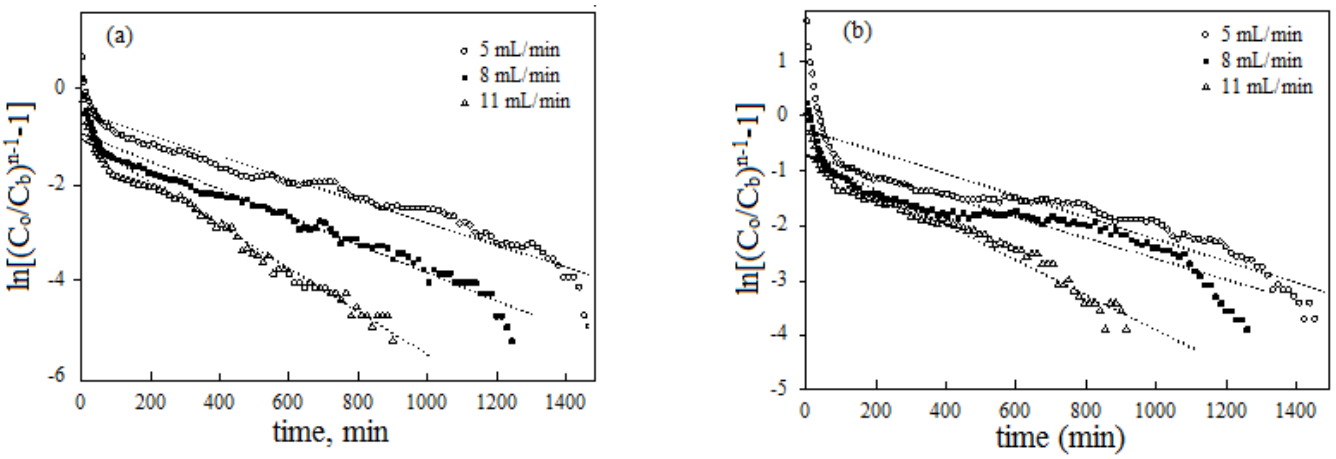

Figure 7. The Clark model's linear form of (a) SRH-R and (b) SB-RS adsorption. Dye concentration = 25 mg/L, pH 4.0 T=30 ºC.

4. Conclusion

The dried eggshell powder-chitosan gel was successfully synthesized and applied as a low-cost and environmentally friendly material for removal of reactive dyes from water. At pH 4.0 and 30 ºC the adsorption process of SRH-R and SB-RS using EPCG reached equilibrium after 60 min with high capacity, which is comparable with activated carbon. The batch adsorption processes on this material are well fitted the Langmuir and Freundlich isotherm equations. When studying the adsorption of this material in a fixed-bed adsorber, the Clark model showed better fitting than by the Bohart – Adam model. This study showed that EPCG can be used as an effective adsorbent for using in water and wastewater treatment applications.

Acknowledgements. The authors gratefully thank Ho Chi Minh City University of Technology and Education for facilities and equipment supports during the completion of this study.

References

[1] Asep Bayu Dani Nandiyanto, *Mor. J. Chem.* 8 **(**2020) 745-761.

[2] C. Zannagui, H. Amhamdi, S. El Barkany, I. Jilal, O. Sundman, A. Salhi, S. Chaouf, M. Abou-Salama, A. El Idrissi, M. Zaghrioui, *Mor. J. Chem.* 8 **(**2020) 332-346.

[3] I. Uzun, *Dyes Pigm.*, 70 **(**2006) 76-83.

[4] S. C. Ihenetu, B. I. Ochule, E. C. Enyoh, F. C. Ibe, A. W. Verla, B. O. Isiuku, *J. Mater. Environ. Sci.*, 11(9) (2020) 1560-1573

[5] J. Carvalho, J. Araujo, F. Castro, *Waste Biomass Valorization*, 2 **(**2011) 157-167.

[6] D. Abunah, C. Onindo, D. Andala, E. Ochoti, *J. Mater. Environ. Sci.*, 10(12) (2019) 1349-1361

[7] S. Chowdhury, P. Das, *Environ. Prog. Sustain. Energy*, 31 **(**2012) 415-425.

[8] W. Tsai, J. Yang, C. Lai, Y. Cheng, C. Lin, C. Yeh, *Bioresour. Technol.*, 97 **(**2006) 488-493.

[9] G. Annadurai, L.Y. Ling, J.-F. Lee, *J. Hazard. Mater.*, 152 **(**2008) 337-346.

[10] N. Pramanpol, N. Nitayapat, *Kasetsart Journal (Natural Science)*, 40 **(**2006) 192-197.

[11] J. Assaoui, A. Kheribech, L. Khamliche, R. Brahmi, Z. Hatim, *Mor. J. Chem.,* 8 **(**2020) 1033-1047**.**

[12] R. Bhaumik, N. Mondal, B. Das, P. Roy, K. Pal, C. Das, A. Baneerjee, *J Chem*, 9 **(**2012) 1457-1480.

[13] M. Foroughi-dahr, M. Esmaieli, H. Abolghasemi, A. Shojamoradi, E. Sadeghi Pouya, *Desalination Water Treat.*, 57 **(**2016) 8437-8446.

[14] A.H. Najafabadi, M. Abdouss, S. Faghihi, *Mater. Sci. Eng. C*, 41 **(**2014**)** 91-99.
[15] H. Pathak, D. Soni, K. Chauhan, *Chemosphere*, 105 **(**2014**)** 126-132.
[16] W. Rudzinski, W. Plazinski, *J. Phys. Chem. B*, 110 **(**2006) 16514-16525.
[17] W. Plazinski, W. Rudzinski, A. Plazinska, *Adv. Colloid Interface Sci.*, 152 **(**2009) 2-13.
[18] A.A. El-Bindary, A. Ismail, E.F. Eladl, *J. Mater. Environ. Sci.*, 10 (2019) 1258-1271.
[19] Y. Yang, G. Wang, B. Wang, Z. Li, X. Jia, Q. Zhou, Y. Zhao, *Bioresour. Technol*, 102 **(**2011) 828-834.
[20] H.A. Chanzu, J.M. Onyari, P.M. Shiundu, *J POLYM ENVIRON*, 20 **(**2012) 665-672.
[21] M. Turabik, *J. Hazard. Mater.*, 158 **(**2008) 52-64.
[22] A. Crhribi, M. Chlendi, *Asian J. Textile*, 1 **(**2011) 161-171.
[23] Y. Al-Degs, M. Khraisheh, S. Allen, M. Ahmad, *J. Hazard. Mater.*, 165 **(**2009) 944-949.
[24] R.M. Clark, *ENVIRON SCI TECHNOL*, 21 **(**1987) 573-580.